CHARACTERIZATION OF HEAT AND MASS TRANSFER IN THE MAT DURING THE HOT PRESSING OF MDF PANELS

Rosilei A. Garcia
M.Sc. Candidate

and

Alain Cloutier†
Professor
Centre de recherche sur le bois
Département des sciences du bois et de la forêt, Université Laval
Québec, QC
Canada G1K 7P4

(Received February 2003)

ABSTRACT

The two objectives of this project were to determine gas permeability of the mat as a function of density, and to characterize panel properties and temperature and gas pressure evolution in the mat during hot pressing as a function of press closing strategy, panel density, and mat moisture content. Panels of 560 × 460 × 16 mm were made in a 600- × 600-mm laboratory press. The manufacturing parameters were the following: press closing strategy of 145, 155, and 165% of the target panel thickness after 30 s of pressing; initial mat moisture content of 10, 12, and 14%; and panel density of 650, 725, and 800 kg m^{-3}. Temperature and gas pressure were measured at the surface and core of the mat. The gas permeability of the panel was measured for panels of uniform densities of 400, 650, 900, and 1150 kg m^{-3}. Gas permeability decreased by a factor of 1000 when panel density increased from 400 to 1150 kg m^{-3}. The flexural properties increased with an increase in mat moisture content and panel density, and a decrease in press closing strategy. The internal bond increased with an increase in mat moisture content and panel density. Thickness swell decreased with an increase of panel density, and increased with an increase in press closing strategy. The time required to reach 100°C in the mat core decreased with a decrease in press closing strategy. The maximum gas pressure in the mat core was proportional to panel density. It also increased with mat moisture content for a press closing strategy of 165% and a panel density of 800 kg m^{-3}.

Keywords: Medium density fiberboard, heat and mass transfer, gas permeability, hot pressing.

INTRODUCTION

The manufacture of wood-based composite panels by means of heat and mechanical pressure is a process known and applied throughout the world. The hot pressing operation is one of the most important and is often the bottleneck of such process. For that reason, various research projects have been performed to improve product performance, reduce pressing time, minimize energy consumption, and maximize wood utilization (Harless et al. 1987; Humphrey and Bolton 1989a; Kamke and Zylkowski 1989). The functions of hot pressing are to consolidate the fiber mat to a desirable panel density and thickness, to cure the resin, and to heat-stabilize the panel so that it remains at the target thickness and density (Hsu 1994). This process involves heat and mass transfer in the mat by conduction and convection. Conduction heat transfer occurs between the press platens and the mat. The water contained in the wood of the surface layers vaporizes because of the fast heating of panel surfaces in contact with the press early in the process. Water vapor movement by filtration is induced towards decreasing vapor pressure in

† Member of SWST.

Wood and Fiber Science, 37(1), 2005, pp. 23–41

the mat core. The vapor carries its latent heat of vaporization and sensible heat, which allow heating of the mat core.

The density profile across thickness is the most important characteristic of MDF panels resulting from the coupled effects of various manufacturing parameters including mat moisture content and structure, and pressing conditions (Harless et al. 1987; Wolcott et al. 1990; Dai and Steiner 1993; Park et al. 1999; Wang and Winistorfer 2000; Winistorfer et al. 2000). The formation of the density profile is a complex phenomenon involving simultaneous heat and mass transfer (Wolcott et al. 1990). These processes are interrelated through the sorption characteristics and viscoelastic behavior of the mat. Kamke and Casey (1988a) measured the conditions inside a flakeboard mat in terms of temperature, moisture content, gas pressure, rate and degree of adhesive cure, density gradient, bond quality, and consequently, the physical and mechanical properties of the resulting products. They noticed that an increase in mat temperature or moisture content decreases the compaction pressure. Humphrey and Bolton (1989b) obtained similar results for a range of mat moisture content between 6% and 26%. In fact, the more humid the wood particles are, the faster the mat becomes plastic. Also, Kamke and Casey (1988a) reported that a greater initial mat moisture content (6 to 15%) increases the rate of temperature rise in the core region, but the maximum temperature may not be greater than the temperature found for a lower mat moisture content. The heat of vaporization, permeability of the mat, and phase equilibrium have an impact on the temperature level. Park et al. (1999) observed an increase in heat transfer by convection with an increasing mat moisture content for three levels: 8%, 11%, and 14%. Kamke and Casey (1988a) and Bolton and Humphrey (1989) state that temperature and gas pressure in the mat are a function of moisture content and press closing time. Their results indicated that little heat transfer occurs in the mat until a significant amount of mat densification has taken place. A faster press closing time results in greater rate of mat densification and this means a rapid buildup of steam pressure in the face region, therefore, a faster rate of convective heat transfer to the core. Smith (1982) observed that the rate of core temperature rise increased with increasing board density and decreasing press closing time from 100 to 30 s. Kamke and Casey (1988b) observed that face and core gas pressures are nearly the same for low platen temperature and low mat moisture content, even though the face and core temperatures are different. High platen temperatures and high mat moisture contents induce a large difference in gas pressure (about 30 kPa) between the face and core layers after press closing and until about 2 min thereafter. High mat moisture content levels result in a panel having better water absorption characteristics and therefore a better dimensional stability. However, the probability of delamination problems and "blows" is higher (Moslemi 1974). Water application to the surface of the mat prior to hot pressing was used by some authors (Johnson and Kamke 1994; Geimer and Kwon 1999). The results obtained by Sosnin (1974) show a higher rate of heat transfer to the core of the panel due to the steam-shock resulting from the vaporization of 0.150 kg/m^2 of water on the mat surface. Also, a reduction of about 20% in the maximum compaction pressure required was observed when heat transfer to the core of the mat was accelerated by the steam-shock effect.

Park et al. (1999) determined the relationship between three pressing variables (face-layer moisture content, platen position, and press closing time) and MDF panel performance. They observed that internal bond strength (IB) increased as the moisture content increased. The optimum conditions obtained for IB strength were face-layer moisture content: 13.4%; press closing time: 3.8 min; and platen position: 111% of the target board thickness of 19.1 mm. The optimum point for the minimum thickness swell (TS) was found to be face-layer moisture content: 13.1%; press closing time: 3.6 min; and platen position: 109.5%. The optimum conditions obtained for the modulus of elasticity (MOE) were face-layer moisture content: 10.0%; closing time: 3.7 min; and platen position: 106.2%. Xu and Suchsland (1998) presented an analytical model to predict the development of the MOE of wood composite panels with a uniform vertical density profile. The simulation showed that the MOE increases linearly with the increase of either panel density or compaction ratio; and the use of a high density wood species results in higher MOE than low density species at the same compaction ratio, but results in lower MOE at the same panel density levels. Panel density is a characteristic of importance due to the influence it has on the physical and mechanical properties of the product. Smith (1982) observed an improvement in MOE and MOR of waferboards with an increase in density. The same author showed that springback increases with an increase in panel density and press closing time. Geimer (1982) and Vital et al. (1980) observed that TS increases with an increase in panel density. However, others have found a decrease in TS with an increase in particleboard density (Hse 1975; and Greubel and Paulitsch 1977).

Because of the significance of convective transfer, the gas permeability of the mat must be known to characterize heat and moisture transfer in the mat during hot pressing. In this context, the transverse permeability K_T determines the flow rate of heat and moisture from the press platens to the mat core. The longitudinal permeability K_L determines the rate of flow from the panel center towards its edges, and hence the heat loss from the panel core and the reduction of internal vapor pressure essential to prevent panel "blows." Together, K_T and K_L control stress relaxation in the pressed product (Bolton and Humphrey 1994). The gas permeability of particleboard in the horizontal direction is always higher than in the vertical direction most likely due to the lower core density (Hata et al. 1993). Lehmann (1972) suggests that K_L is 5 to 10 times greater than K_T at a given density. Bowen (1970) suggests that K_L is one order of magnitude greater than K_T at a given density. Denisov et al. (1975) and Zuban (1969) suggest differences sometimes greater than two orders of magnitude, with the differences being greater at higher densities. Bolton and Humphrey (1994) suggested that as panel density increases, permeability must decrease. Over the density range 510 to 740 kg m^{-3}, Bowen (1970) observed a slightly curvilinear decrease of K_T with an increase in density. Denisov et al. (1975) and Lehmann (1972) reported similar results. However, Lehmann (1972) observed a linear relationship in the density range 230 to 980 kg m^{-3}. Hata et al. (1993) reported similar results for particleboard produced by steam-injection pressing (Fig. 1). Also, Sokunbi (1978) found a decrease of gas permeability from 64×10^{-15} m^2 to 2×10^{-15} m^2 with an increase in particleboard density from 425 to 875 kg m^{-3}. The increase in the rate of core temperature rise with an increasing panel density and decreasing press closing time reported by Smith (1982) can be explained by the gas permeability. As panel density increases, gas permeability decreases which allows steam pressure buildup in the panel and the resulting temperature rise. A short press closing time allows a more permeable mat core because of lower core densification.

Lihra et al. (2000) measured the apparent gas permeability k_g^* for balsam fir (*Abies balsamea*) based on Darcy's law applied to gas flow through wood as described by Siau (1995):

$$k_g^* = \frac{QL}{A\Delta P}\frac{P}{\overline{P}} \tag{1}$$

where k_g^* is the apparent gas permeability with slip flow ($m_{gas}^3\ m_{wood}^{-1}\ s^{-1}\ Pa^{-1}$); Q is the volumetric gas flow rate ($m_{gas}^3\ s^{-1}$); L is the length in the flow direction (m_{wood}); A is the cross-

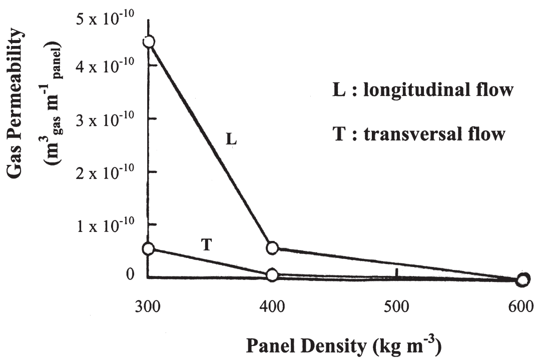

FIG. 1. Effect of panel density on gas permeability of particleboards (adapted from Hata et al. 1993).

sectional area of the specimen (m_{wood}^2); ΔP is the pressure differential across the specimen (Pa); P is the pressure at which Q is measured (Pa); and $\overline{P}$ is the average pressure across the specimen (Pa).

The apparent gas permeability k_g^* includes Knudsen diffusion, also called slip flow. When a gas flows through a capillary whose diameter is in the same order of magnitude as the average free path between the gas molecules, slip flow becomes significant and must be considered in the permeability measurement. The gas permeability corrected for slip flow may be obtained from the Klinkenberg equation (Siau 1995):

$$k_g^* = k_g\left(1+\left(\frac{b}{\overline{P}}\right)\right) \tag{2}$$

with

$$b = 3.8\lambda\left(\frac{\overline{P}}{r}\right) \tag{3}$$

and

$$\lambda = \frac{2\mu}{\overline{P}}\sqrt{\frac{RT}{M}} \tag{4}$$

where k_g is gas permeability corrected for slip flow ($m_{gas}^3\ m_{wood}^{-1}\ s^{-1}\ Pa^{-1}$), b is the Klinkenberg factor (Pa), λ is the average free path between gas molecules (m), r is the diameter of the capillary, μ is the viscosity of the fluid used to determine (Pa s), R is the universal gas constant (8.31 J $mol^{-1}K^{-1}$), T is the absolute temperature (K), and M is the molecular weight of the gas (kg mol^{-1}). The apparent gas permeability, k_g^*, is a linear function of the reciprocal average pressure (Eq. 2). In fact, the gas permeability k_g represents the "true" gas permeability corrected for slip flow and can be found graphically from the intercept of a plot of k_g^* against $1/\overline{P}$ (Fig. 2). The gas permeability k_g is by definition the permeability of the solid to the permeating gas. By introducing the viscosity of the gas, the intrinsic permeability of the solid is obtained by:

$$K = k_g\mu \tag{5}$$

where K = intrinsic permeability ($m_{gas}^3\ m_{wood}^{-1}$).

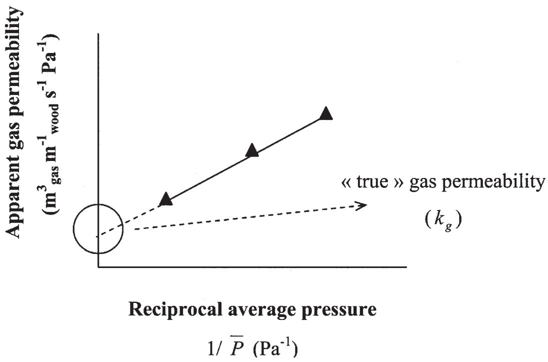

FIG. 2. Typical plot of the apparent gas permeability against the reciprocal pressure (adapted from Lihra et al. 2000).

K is independent of the permeating gas used and is only a function of the porous structure of the body.

Recently, Perré and Agoua (2001) published results on the gas permeability of MDF as a function of panel density. They found K values decreasing linearly from 4×10^{-12} to 2.5×10^{-13} m^2 for panel densities varying from 250 to 750 kg m^{-3}. Unfortunately, the authors do not specify if a density profile was present across the thickness of the samples used to perform the measurements.

Given the importance of hot pressing in MDF manufacturing, it is fundamental to characterize heat and mass transfer in the mat during that process and its impact on panel properties. Therefore, the objectives of this project were 1) to determine gas permeability of the MDF mat as a function of panel density, and 2) to characterize the properties of MDF panels and temperature and gas pressure evolution in the MDF mat during hot pressing as a function of press closing strategy, panel density and mat moisture content.

MATERIALS AND METHODS

Manufacturing of MDF panels and experimental design

Softwood fibers (90% black spruce and 10% balsam fir) were obtained from Uniboard Canada Inc., Panneaux MDF La-Baie plant in

Ville-de-la-Baie, Québec, Canada. MDF panels measuring 560 × 460 × 16 mm were manufactured using a 600- × 600-mm laboratory press available at the Département des sciences du bois et de la forêt, Université Laval, Québec, Canada. The target panel densities were 650, 725, and 800 kg m^{-3}, and the target panel thickness was 16.0 mm. The panels were produced at initial mat moisture contents of 10, 12, and 14% using three press closing strategies: 30 s until 145, 155, and 165% of the target panel thickness was reached for a total of 2.5 min of pressing in each case. Three replicates were produced at each set of treatment combination. The other manufacturing parameters are presented in Table 1. After manufacturing, the panels were conditioned to 20°C and 60% RH for 72 h.

A 3^3 factorial experimental design was used. The 27 treatment combinations and 3 replications resulted in a total of 81 panels. The modulus of elasticity (MOE), modulus of rupture (MOR), internal bond (IB) and thickness swell (TS) were determined according to the procedures described in the ANSI A208.2-1994 (1994) and ASTM D1037-96a (1996) standards. The heat transfer was characterized by measuring temperature at the surface using a type K thermocouple, and temperature in the core using a temperature and pressure probe developed by Alberta Research Council. The time required to reach 100°C at the mat core (T_{100}) and the maximum temperature difference between the surface and the core (ΔT_{max}) were used to characterize heat transfer. The maximum gas pressure in the core (GP_{max}) and the maximum gas pressure difference between the surface and the core (ΔGP_{max}) were used to analyze mass transfer.

Gas permeability

Panels manufacturing.—The MDF panels used for gas permeability measurements were produced by cold pressing. The press was closed and once the panel target thickness was reached, the heating of the press platens was started. Once the core reached 120°C, the mat was heated for 2.5 min to cure the UF resin. The total pressing cycle was about 55 min. This strategy allowed to obtain an homogeneous density profile across panel thickness to prevent the interference of density variation in gas permeability measurement.

Gas permeability measurements.—MDF gas permeability was measured with medical air using an apparatus developed in our laboratory by Lihra et al. (2000) (Fig. 3a). Gas permeability was measured on panels of 4 density levels: 400, 650, 900, and 1150 kg m^{-3} and 3 replications for

TABLE 1. *MDF panels manufacturing parameters.*

Parameter	Condition
Board size	560 × 460 × 16 mm
Mat moisture content	10, 12, 14% (based on oven-dry wood)
Target panel density	650, 725, 800 kg m^{-3}
Wax content	1% (based on oven-dry wood)
Resin type	Commercial Urea Formaldehyde, Neste Resin Canada Inc.
Resin solid content	65%
Resin viscosity	0.335 Pa s
Resin gel time	> 15 minutes
Resin content	14% (based on ovn-dry wood)
Catalyst used	Solution of NH_4Cl at 30%
pH after catalyst	7.0
Press platen temperature	210°C
Total press closing time	2:30 minutes
Curing time	2:30 minutes
Press opening time	1 minute
Pressing strategy	145, 155, 165% of target panel thickness after 30 s

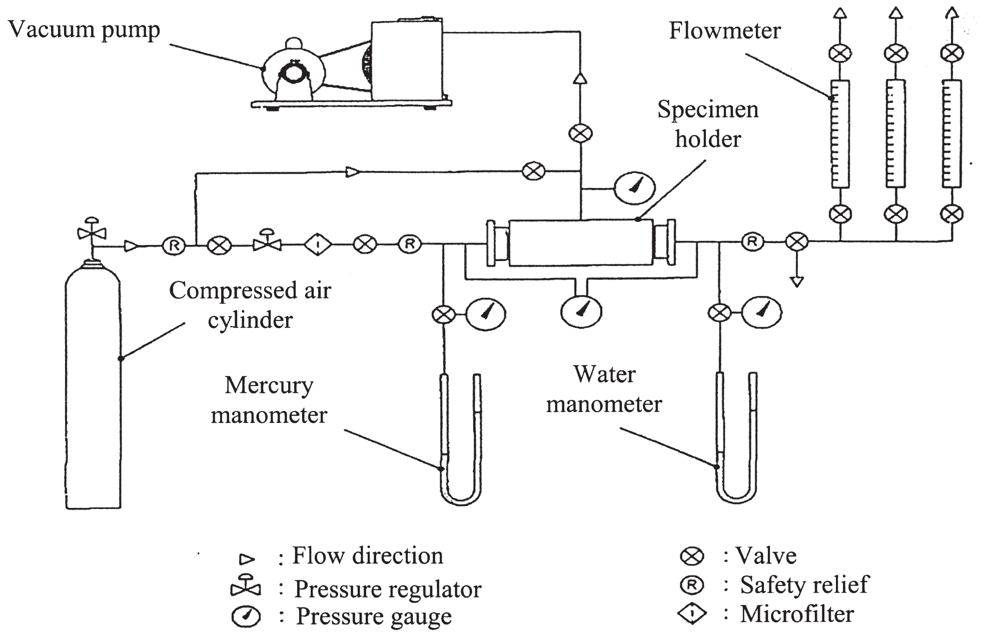

(a)

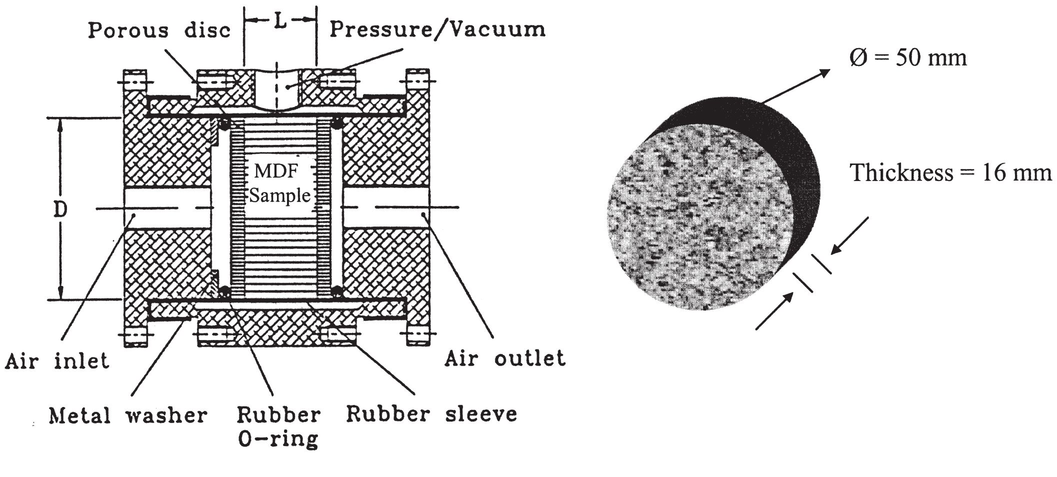

(b)

FIG. 3. (a) Apparatus used to gas permeability measurements. (b) Specimen holder for gas permeability measurements and schematic representations of the specimens (adapted from Lihra et al. 2000).

a total of 12 panels. For each panel, four discs of 50 mm in diameter and 16 mm in thickness were used for a total of 48 test specimens (Fig. 3b). The final cut of the end surfaces was made with a microtome to obtain the highest permeability values possible. Silicon seal was applied on the edge of the samples to provide a tight seal with the rubber sleeve. A basswood disc (*Tilia americana*) was placed on the inlet and outlet sides of the specimen to distribute the air flow over the cross-section and prevent end-effects. The resistance to gas flow of the disks was negligible because of basswood high longitudinal gas permeability. The apparent gas permeability k_g^* was measured at three pressure levels. A one-way classification analysis of variance was used to compare the gas permeability obtained for the 4 density levels.

RESULTS AND DISCUSSION

Effect of panel density on gas permeability

Typical density profiles of the MDF panels produced for gas permeability measurements are presented in Figs. 4 and 5. The cold pressing strategy resulted in relatively flat density profiles, although it was more difficult to obtain for the higher densities. This can be explained by an heterogeneous heat transfer during the heating of the press platens resulting in the development of a density profile. Nevertheless, these panels were used to produce gas permeability specimens with a reasonably homogeneous density profile.

Figure 6 shows the results obtained for gas permeability as a function of panel density. As suggested by Bolton and Humphrey (1994), gas permeability decreases with an increase in panel density. Figure 6 shows a curvilinear decrease of $\log_{10}$ K with an increase in panel density. The analysis of variance shows that density has a significant impact at the 99% probability level on gas permeability in the range of 400 to 1150 kg m^{-3} (F_{value} = 771.09). The average intrinsic gas permeability values were 1.1×10^{-12} m^3_{gas} m^{-1}_{panel} at 400 kg m^{-3}; 7.0×10^{-13} m^3_{gas} m^{-1}_{panel} at 650 kg m^{-3}; 3.4×10^{-14} m^3_{gas} m^{-1}_{panel} at 900 kg m^{-3}; and 3.4×10^{-15} m^3_{gas} m^{-1}_{panel} at 1150 kg m^{-3}. The comparison between means presented in Table 2 shows that all mean K values were significantly different. A difference of three orders of magnitude was found for K between 400 and 1150 kg m^{-3}. The increase in gas permeability following a decrease in density is due to the increasing proportion of voids in the material. Our results show a similar trend as those found by Hata et al. (1993), who observed a decrease in gas permeability with an increase in particleboard density in the 300 to 600 kg m^{-3} range. The transverse gas permeability values they found are in the same order of magnitude as those found in the current study. However, a density profile could have been present in the specimens used by Hata et al. (1993), even though steam injection was used to produce their particleboards. Therefore, a comparison between the results obtained in both studies should be made with care. The intrinsic gas permeability results we obtained (Fig. 6) are in agreement with the results obtained by Perré and Agoua (2001) for MDF in the density range 250 to 750 kg m^{-3}.

Effect of pressing parameters on mechanical and physical properties

The results of the analysis of variance for the 8 variables considered are presented in Table 3. A discussion follows for each variable studied.

Modulus of elasticity and modulus of rupture.—The results obtained for the modulus of elasticity (MOE) and modulus of rupture (MOR) for all the combinations are presented in Tables 4 and 5, respectively. The analysis of variance shows that press closing strategy, mat moisture content, and panel density have a significant impact on MOE and MOR. No interactions were found to be significant. The results obtained for MOE and MOR as a function of press closing strategy, mat moisture content, and panel density are shown in Figs. 7 to 10, respectively. For both MOE and MOR, the best performance was obtained with a press closing strategy of 145% of target panel thickness. This could be expected because a higher densification of the surface can occur with a faster press closing.

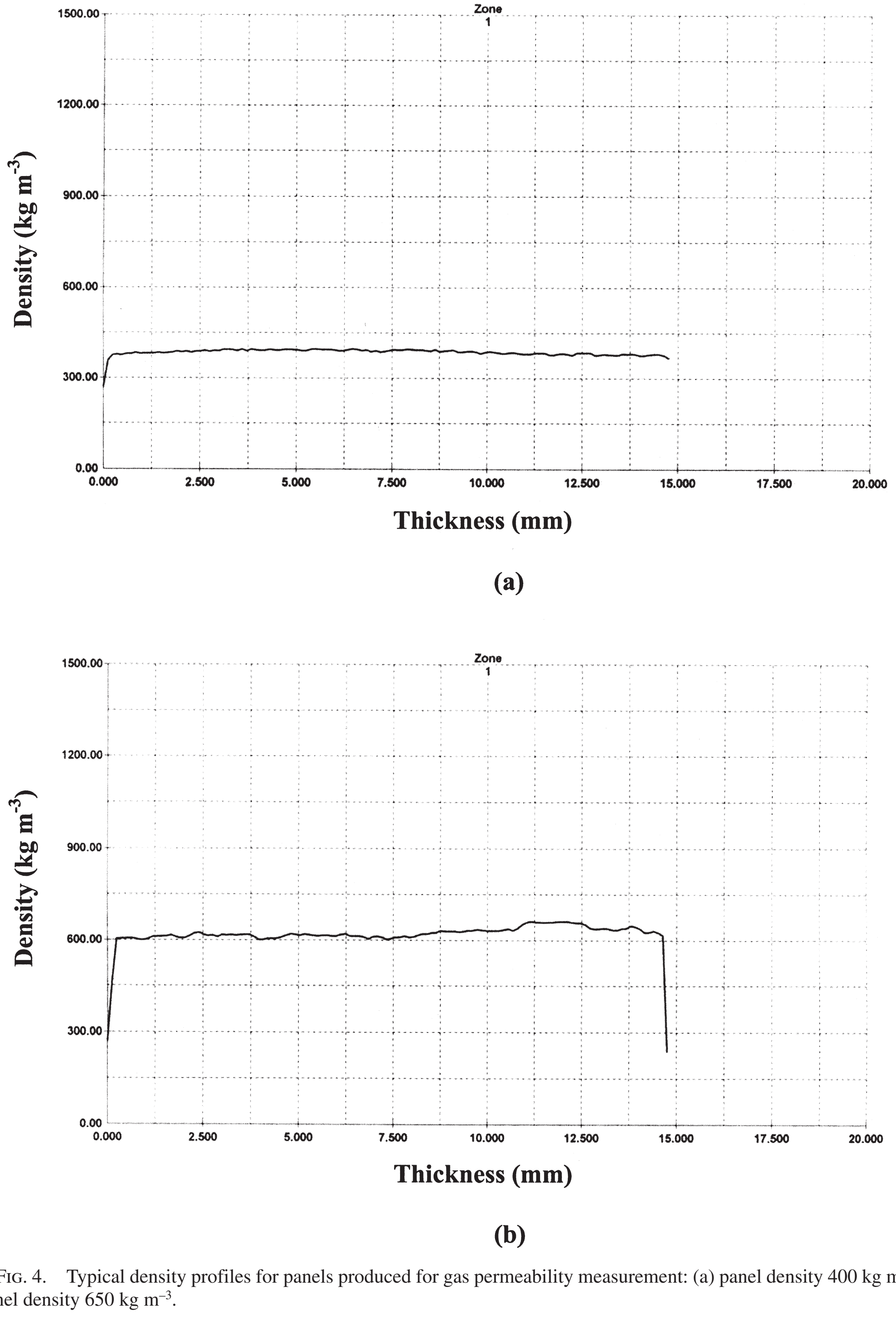

FIG. 4. Typical density profiles for panels produced for gas permeability measurement: (a) panel density 400 kg m^{-3}, (b) panel density 650 kg m^{-3}.

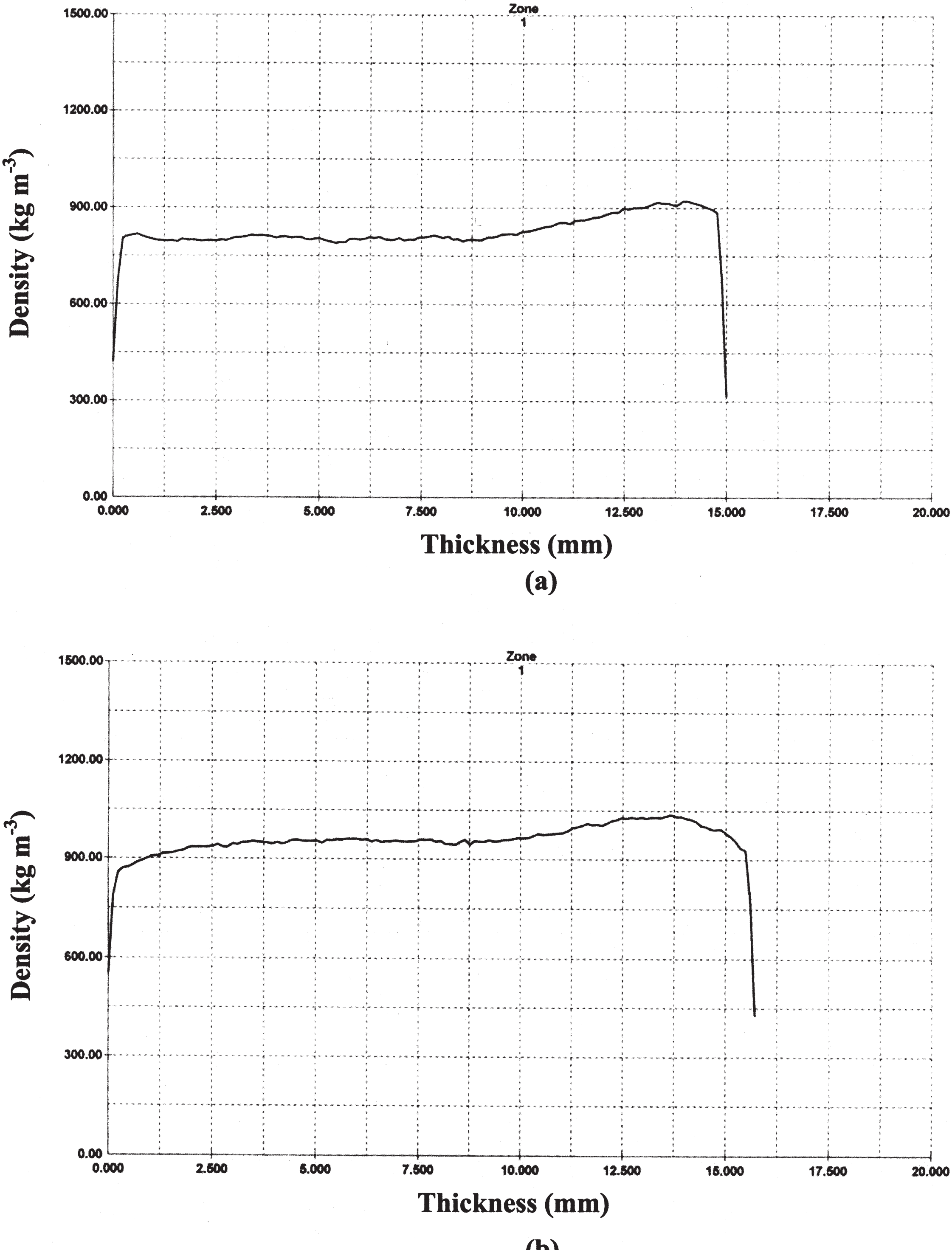

FIG. 5. Typical density profiles for panels produced for gas permeability measurement: (a) panel density 900 kg m^{-3}, (b) panel density 1150 kg m^{-3}.

These results are in agreement with those found by Park et al. (1999), who observed an increase in MOE with a decrease of press closing strategy. A typical density profile for 145% of target panel thickness is presented in Fig. 8. The profile is typical of industrial MDF panels with a high density at the surface and a lower homogeneous density in the core.

The results show a significant increase of both MOE and MOR when using a mat moisture content of 14% as compared to 10 and 12% (Fig. 9).

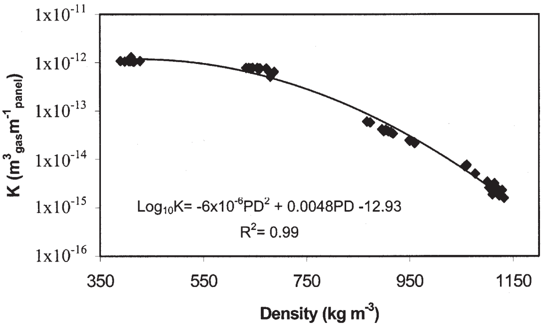

FIG. 6. Gas permeability as a function of MDF density.

This can be explained by the higher densification of the surface due to the higher plasticization of wood fibers at higher moisture content. As expected, MOE and MOR increase with an increase in panel density (Fig. 10). These results are in agreement with those found by Xu and Suchsland (1998) which showed that the MOE increases linearly with the increase in panel density. The optimum conditions determined for MOE and MOR are a press closing strategy of 145% of target panel thickness, a mat moisture content of 14% and a panel density of 800 kg m^{-3}.

Internal bond strength.—The analysis of variance shows that mat moisture content and panel density have a significant impact on internal bond strength (IB). Table 6 presents the results obtained for IB for all combinations. The results obtained for IB as a function of mat moisture content are presented in Fig. 11a. This figure shows a maximum IB obtained at 14% MMC significant at the 99% probability level. The average IB values obtained for 10 and 12% MMC were not significantly different to the exception of the values obtained at 650 kg m^{-3}. This positive impact of MMC on IB can be explained by a faster heat

TABLE 2. *Duncan's multiple range test for intrinsic gas permeability.*

Duncan Grouping	Mean K ($m^3_{gas} m^{-1}_{panel}$)	($\log_{10}$ K)[1]	Std Dev. ($\log_{10}$ K)	N	Nominal Density (kg m^{-3})
A	1.1×10^{-12}	–11.96333	0.02	12	400
B	7.0×10^{-13}	–12.14250	0.09	12	650
C	3.4×10^{-14}	–13.46083	0.15	12	900
D	3.4×10^{-15}	–14.48167	0.25	12	1150

[1] Corresponding values of $\log_{10}$ K of the mean intrinsic gas permeability ($m^3_{gas} m^{-1}_{panel}$).

TABLE 3. *Results of the analysis of variance* (F *values).*

Source of Variation	Physical and Mechanical Properties				Temperature and Gas Pressure			
	MOE	MOR	IB	TS	T_{100}	ΔT_{max}	GP_{max}	ΔGP_{max}
PCS	38.3**	22.9**	0.4 ns	4.3*	28.8**	0.07 ns	0.9 ns	0.8 ns
MMC	22.2**	18.5**	10.9**	2.3 ns	16.7**	1.1 ns	3.7*	1.7 ns
PD	267.8**	269.6**	42.4**	22.3**	0.02 ns	0.7 ns	263.3**	5.0 *
PCS*MMC	0.3 ns	0.1 ns	2.3 ns	0.2 ns	1.1 ns	0.03 ns	0.3 ns	0.9 ns
PCS*PD	2.3 ns	2.2 ns	1.1 ns	0.9 ns	0.4 ns	0.1 ns	1.1 ns	0.3 ns
MMC*PD	1.5 ns	1.4 ns	7.6**	0.8 ns	1.3 ns	0.08 ns	1.7 ns	0.2 ns
PCS*MMC*PD	0.9 ns	0.8 ns	0.2 ns	0.4 ns	0.5 ns	0.2 ns	0.3 ns	NA

** significant at 99% probability level; * significant at 95% probability level; and ns: not significant.

PCS: Press closing strategy; MMC: mat moisture content; and PD: panel density. MOE: modulus of elasticity; MOR: modulus of rupture; IB: internal bond strength; TS: thickness swelling; T_{100}: time required to reach 100°C in the mat core; ΔT_{max}: maximum temperature difference reached between mat surface and core; GP_{max}: maximum gas pressure in the mat core; ΔGP_{max}: maximum difference in gas pressure between mat surface and core; NA: not analyzed.

TABLE 4. *Results obtained for modulus of elasticity (MOE) in MPa for all combinations.*

Mat moisture content (%)	Press closing strategy (% of target panel thickness)								
	145			155			165		
	Nominal panel density (kg m^{-3})								
	650	725	800	650	725	800	650	725	800
10	1726	2557	2985	1476	2252	2884	1444	1924	2481
	(247)	(327)	(449)	(182)	(226)	(149)	(200)	(42)	(39)
12	1792	2423	3534	1817	2351	3174	1634	2117	2730
	(216)	(53)	(428)	(42)	(214)	(210)	(139)	(166)	(160)
14	2131	2868	3471	2040	2442	3274	1711	2334	2773
	(211)	(110)	(52)	(139)	(113)	(128)	(144)	(200)	(188)

ANSI A208.2–1994/ MD Class: MOE (modulus of elasticity) 2400 MPa. Standard deviation for three replicates of each combination is given in brackets.

TABLE 5. *Results obtained for modulus of rupture (MOR) in MPa for all combinations.*

Mat moisture content (%)	Press closing strategy (% of target panel thickness)								
	145			155			165		
	Nominal panel density (kg m^{-3})								
	650	725	800	650	725	800	650	725	800
10	15.1	23.1	27.0	14.0	21.1	26.5	13.6	17.8	22.9
	(1.8)	(2.5)	(3.5)	(2.8)	(2.1)	(0.8)	(2.5)	(1.1)	(1.1)
12	14.7	21.9	30.7	16.0	20.3	27.9	14.3	19.0	24.9
	(1.8)	(1.5)	(3.9)	(0.7)	(1.9)	(0.9)	(0.7)	(0.2)	(0.6)
14	17.8	25.6	31.6	18.0	21.9	31.5	15.1	20.9	27.3
	(2.6)	(0.9)	(1.4)	(2.1)	(0.5)	(2.1)	(1.6)	(2.2)	(2.8)

ANSI A208.2–1994/ MD Class: MOR (modulus of rupture) 24 MPa. Standard deviation for three replicates of each combination is given in brackets.

transfer to the core due to the higher mat moisture content resulting in a better resin cure. These results are in agreement with those found by Park et al. (1999), who observed an increase in IB strength with an increase in moisture content. As for MOE and MOR, the IB is proportional to panel density (Fig. 11b). The optimum conditions observed for IB strength were the following: press closing strategy of 145% of target panel thickness; mat moisture content of 14%; and panel density of 800 kg m^{-3}. A highly significant interaction was observed between MMC and PD for IB strength. This is due to the decrease in IB occurring when panel density increased from 725 to 800 kg m^{-3} at 14% MMC only. This can be explained by the negative impact of the higher gas pressure in the core on resin cure resulting from the combined effect of the higher MMC and the lower gas permeability at 800 kg m^{-3}.

Thickness swell.—The analysis of variance shows that press closing strategy and panel density have a significant impact on thickness swell (TS). No interactions were found between pressing parameters. The results obtained for TS for all combinations are presented in Table 7. The results show a significant increase of TS with a decrease in panel density (Fig. 12a). These results are similar to those found by Hse (1975) and Greubel and Paulitsch (1977). This result can be attributed to the lower panel porosity obtained for higher panel density. This reduces water penetration in the panel and decreases TS over the 24-h duration of the TS test. However, over a long period of time, a higher TS can be expected for a high density panel. Thickness swell significantly increased as PCS increased (Fig. 12b). This can be explained by the higher porosity due to the lower surface density resulting from the slower press closing. The impact of

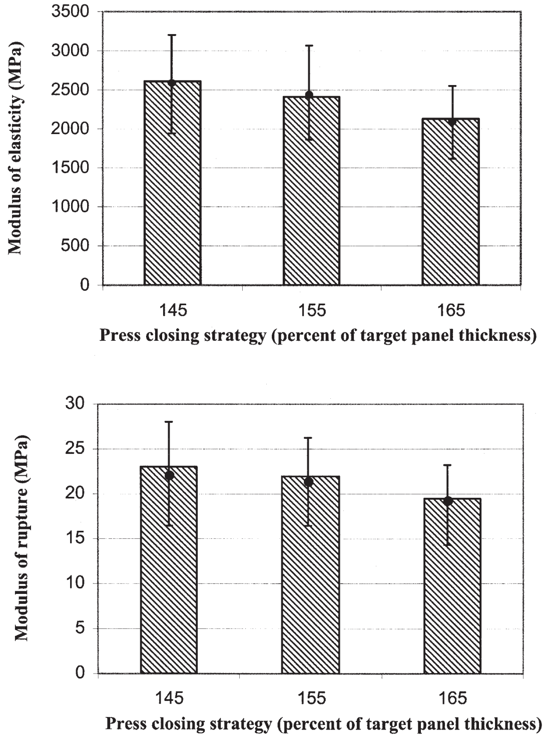

FIG. 7. Average modulus of elasticity (MOE) and modulus of rupture (MOR) as a function of press closing strategy (ANSI A208.2-1994/ MD Class: MOE 2400 MPa; and MOR 24 MPa). The standard deviation is shown for each average value.

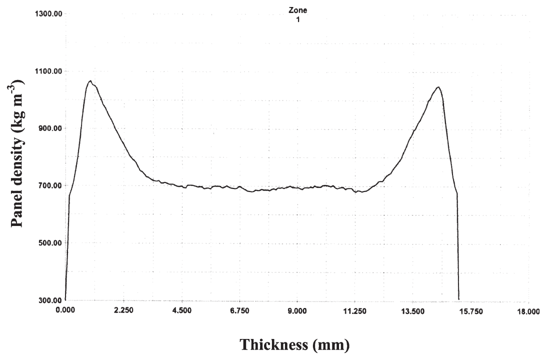

FIG. 8. Typical density profile for press closing strategy of 145 % of target panel thickness, mat moisture content of 10 %, and panel density of 800 kg m^{-3}.

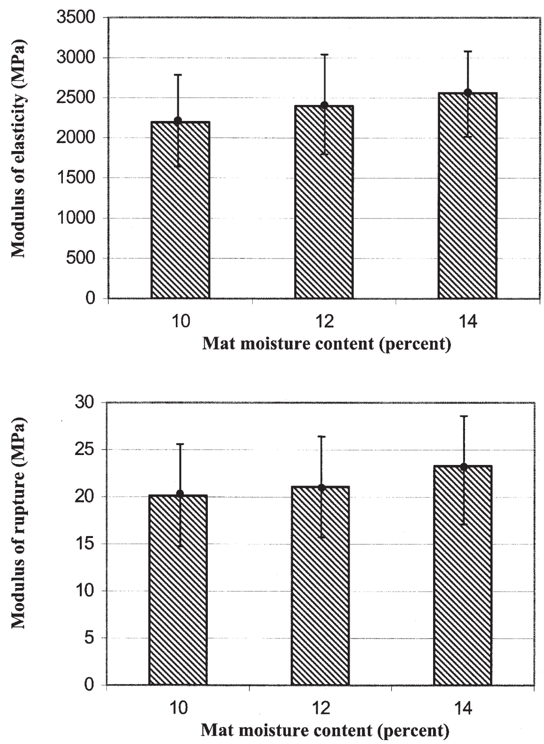

FIG. 9. Average modulus of elasticity (MOE) and modulus of rupture (MOR) as a function of mat moisture content (ANSI A208.2–1994/ MD Class: MOE 2400 MPa; and MOR 24 MPa). The standard deviation is shown for each average value.

this is a faster water penetration and therefore a higher TS.

Effect of pressing parameters on temperature and gas pressure evolution in the mat

Temperature.—Heat transfer in the MDF mat was characterized by two parameters: the time required to reach 100°C in the mat core (T_{100}) and the maximum temperature difference reached between mat surface and mat core (ΔT_{max}). The analysis of variance shows that PCS and MMC have a significant impact on T_{100}. No interaction effect between the factors studied was significant. A typical curve of temperature and gas pressure evolution in the mat during hot pressing is presented in Fig. 13. The surface reaches 100°C about 75 s before the core. The core temperature does not go beyond 115°C and ΔT_{max} occurs during the first 100 s. The results for T_{100} for all combinations are presented in Table 8. The time to reach 100°C decreased with a decrease in PCS (Fig. 14a). Therefore, the faster the initial press closing is performed, the faster the core is heated. This is in agreement with the results reported by Park et al. (1999).

Typical curves illustrating mat core temperature against time for the three MMCs considered

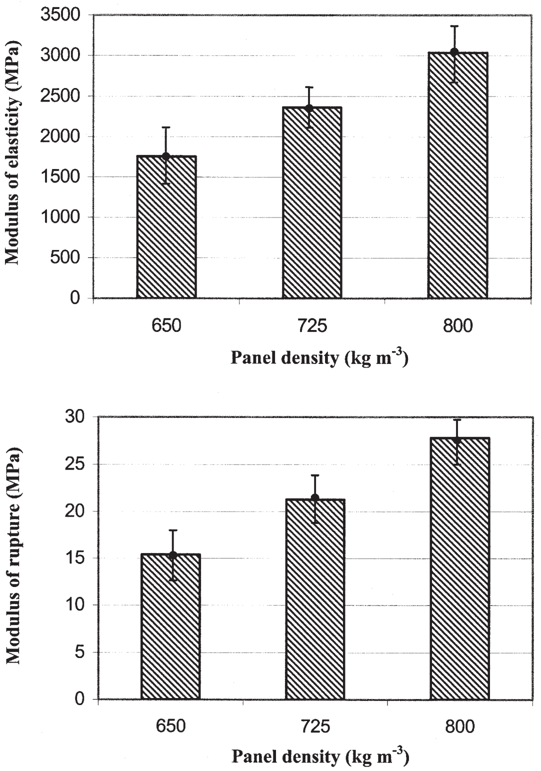

FIG. 10. Average modulus of elasticity (MOE) and modulus of rupture (MOR) as a function of panel density (ANSI A 208.2–1994/ MD Class: MOE 2400 MPa; and MOR 24 MPa). The standard deviation is shown for each average value.

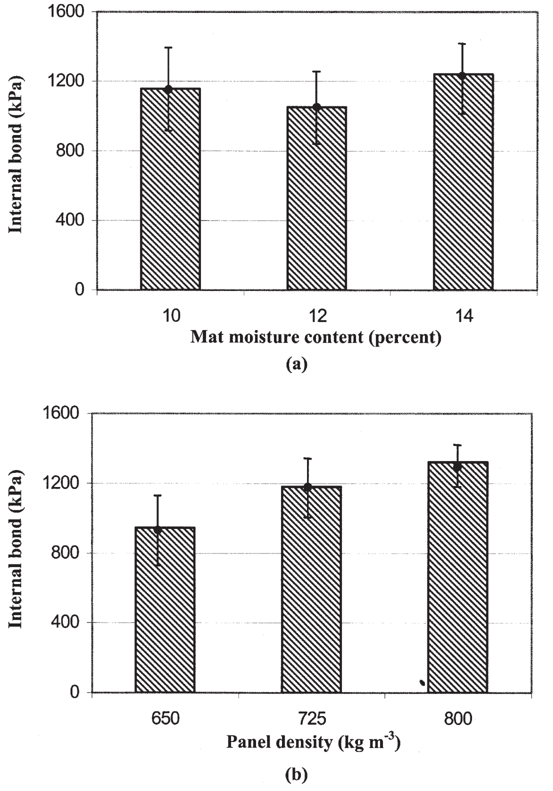

FIG. 11. (a) Average internal bond strength as a function of mat moisture content. (b) Average internal bond strength as a function of panel density (ANSI A208.2–1994/ MD Class: IB 600 kPa). The standard deviation is shown for each average value.

TABLE 6. *Results obtained for internal bond strength (IB) in kPa for all combinations.*

	Press closing strategy (% of target panel thickness)								
	145			155			165		
Mat moisture content (%)	Nominal panel density (kg m^{-3})								
	650	725	800	650	725	800	650	725	800
10	827	1125	1313	1012	1036	1395	962	1241	1499
	(316)	(104)	(87)	(100)	(107)	(148)	(178)	(61)	(129)
12	790	1119	1406	849	1073	1336	681	957	1239
	(137)	(126)	(8)	(84)	(112)	(96)	(39)	(45)	(101)
14	1045	1377	1274	1240	1374	1205	1113	1326	1211
	(238)	(69)	(295)	(156)	(207)	(175)	(159)	(201)	(99)

ANSI A208.2–1994/ MD Class: IB (internal bond strength) 600 kPa. Standard deviation for three replicates of each combination is given in brackets.

are presented in Fig. 14b. Our results show an impact of MMC on T_{100}. A MMC of 10% resulted in a lower T_{100} than for MMCs of 12 and 14%. This result was not expected and is most likely due to an uncontrolled parameter or to the higher energy required to heat up mats at higher moisture contents. The actual heating rate depends of the heating capacity of the hot press. Further work is needed to clarify this aspect of the study. Park et al. (1999) observed a significant decrease of the time to reach 120°C in the mat core with an increase of the surface layers moisture content from 8 to 14%. Humphrey and Bolton (1989a) also observed a higher core temperature increasing rate with a higher mat moisture content. This was also expected in this study but our results do not allow to make such a conclusion.

The results obtained for ΔT_{max} are presented in Table 9. Curves of average ΔT_{max} against time for the three densities considered are presented in Fig. 15. The higher ΔT_{max} values occur between 50 and 200 seconds of pressing with a maximum at about 120 s, corresponding to the beginning of the temperature rise in the panel

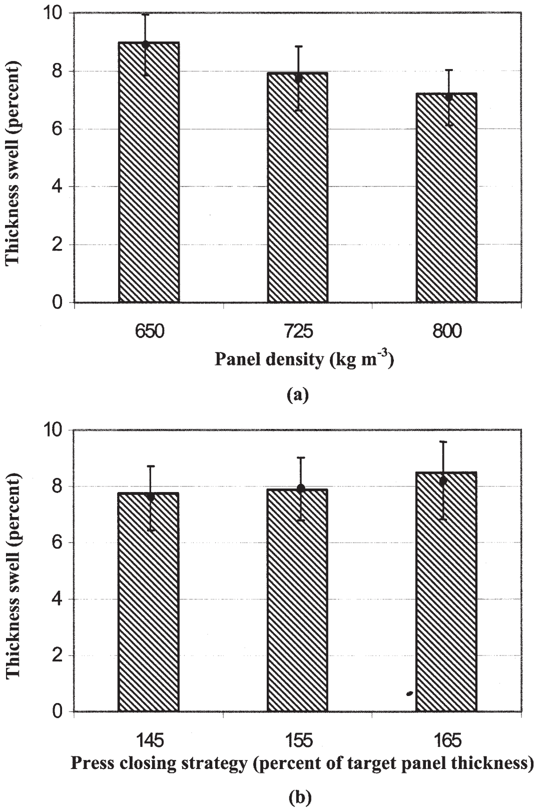

FIG. 12. (a) Average thickness swell as a function of panel density. (b) Average thickness swell as a function of press closing strategy (ASTM D1037-96a: 8% for particleboard products). The standard deviation is shown for each average value.

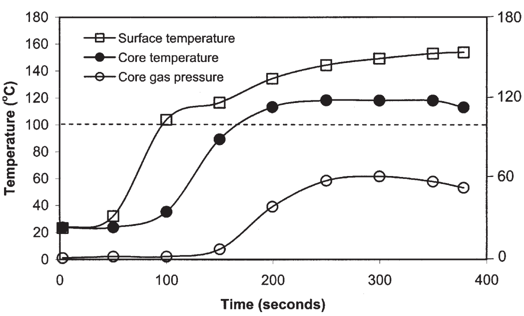

FIG. 13. Typical curves of temperature and gas pressure evolution during hot pressing (press closing strategy: 145% of target panel density; mat moisture content: 10% and panel density: 725 kg m^{-3}).

TABLE 7. *Results obtained for thickness swell (TS) in percentage for all combinations.*

Mat moisture content (%)	Press closing strategy (% of target panel thickness)								
	145			155			165		
	Nominal panel density (kg m^{-3})								
	650	725	800	650	725	800	650	725	800
10	9.0	7.8	7.0	8.8	8.4	7.3	9.7	8.	7.5
	(1.5)	(1.7)	(1.1)	(0.9)	(1.9)	(1.2)	(1.4)	(1.8)	(1.3)
12	8.6	7.6	7.2	9.4	7.9	7.1	10.2	8.7	7.1
	(0.2)	(0.8)	(0.5)	(0.6)	(0.2)	(0.9)	(0.1)	(0.6)	(0.3)
14	8.1	7.0	7.4	7.8	7.8	6.6	9.2	7.9	7.6
	(0.8)	(1.3)	(0.7)	(0.6)	(0.3)	(0.3)	(0.9)	(0.1)	(0.7)

ASTM D1037-96a: thickness swell (TS) 8% for particleboard products. Standard deviation for three replicates of each combination is given in brackets.

TABLE 8. *Results obtained for T_{100} (s) for all combinations.*

Mat moisture content (%)	Press closing strategy (% of target panel thickness)								
	145			155			165		
	Nominal panel density (kg m^{-3})								
	650	725	800	650	725	800	650	725	800
10	166	167	165	166	168	169	187	177	195
	(11)	(18)	(7)	(22)	(6)	(9)	(22)	(40)	(8)
12	187	183	175	201	187	191	216	218	205
	(8)	(6)	(19)	(5)	(13)	(11)	(10)	(5)	(16)
14	170	172	169	185	193	189	198	209	221
	(9)	(17)	(0)	(8)	(18)	(15)	(15)	(15)	(5)

T_{100}: time required to reach 100°C in the mat core (seconds). Standard deviation for three replicates of each combination is given in brackets.

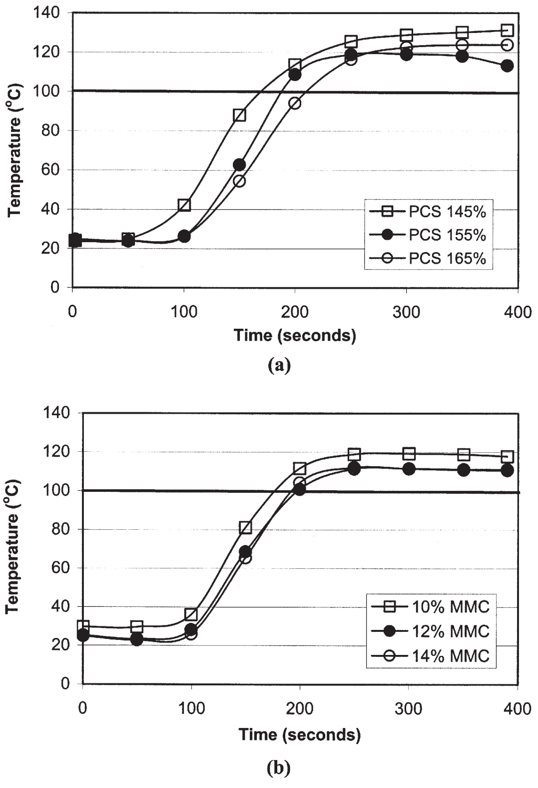

FIG. 14. (a) Example of core temperature evolution as a function of press closing strategy during hot pressing (treatment combinations: PCS 145%: 800 kg m^{-3} PD and 14% MMC; PCS 155%: 800 kg m^{-3} PD and 14% MMC; PCS 165%: 800 kg m^{-3} PD and 14% MMC). (b) Example of core temperature evolution as a function of mat moisture content during hot pressing (treatment combinations: 10% MMC: 725 kg m^{-3} PD and 155% PCS; 12% MMC: 650 kg m^{-3} PD and 155% PCS; 14% MMC: 650 kg m^{-3} PD and 155% PCS). Panel density has no significant impact.

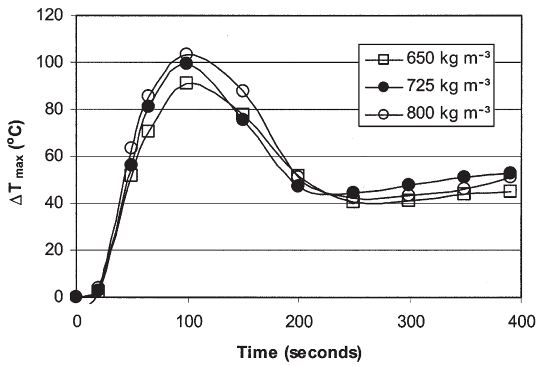

FIG. 15. Average temperature difference between mat surface and core (ΔT_{max}) as a function of panel density.

core. As shown in Table 3, none of the parameters studied had a significant effect on ΔT_{max}. However, an increase in panel density resulted in a slight increase of ΔT_{max} (Fig. 15), although not statistically significant. This trend can be attributed to the higher vapor pressure in the core resulting from the decreasing gas permeability of the mat as density increases. Further experiments are required to assess this effect.

Gas pressure.—Mass transfer in the mat was characterized by two parameters: first, the maximum gas pressure in the mat core (GP_{max}) (Table 10), and second the maximum difference in gas pressure between mat surface and core (ΔGP_{max}). Panel density and mat moisture content had a linear significant effect on GP_{max}

TABLE 9. *Results obtained for ΔT_{max} (°C) for all combinations.*

Mat moisture content (%)	Press closing strategy (% of target panel thickness)								
	145			155			165		
	Nominal panel density (kg m^{-3})								
	650	725	800	650	725	800	650	725	800
10	85	96	93	88	97	101	87	75	98
	(41)	(31)	(36)	(39)	(44)	(41)	(59)	(51)	(34)
12	96	103	111	94	100	113	101	102	104
	(37)	(4)	(22)	(34)	(27)	(21)	(50)	(46)	(29)
14	105	116	102	99	112	106	82	107	121
	(34)	(31)	(34)	(37)	(32)	(34)	(44)	(39)	(33)

ΔT_{max}: maximum temperature difference reached between mat surface and mat core (°C). Standard deviation for three replicates of each combination is given in brackets.

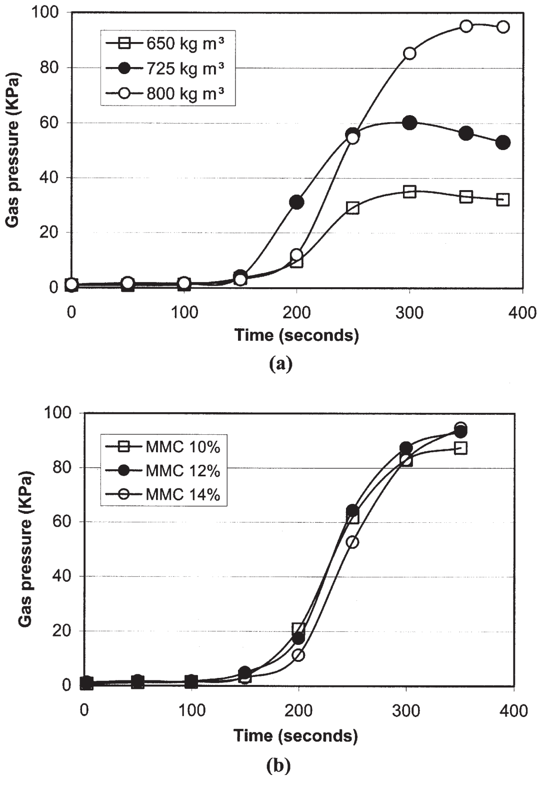

FIG. 16. (a) Example of core gas pressure evolution as a function of panel density (treatment combinations: 650 kg m^{-3}: 165% PCS and 10% MMC; 725 kg m^{-3}: 155% PCS and 10% MMC; 800 kg m^{-3}: 165% PCS and 12% MMC). (b) Example of core gas pressure evolution as a function of mat moisture content (treatment combinations: 10% MMC: 800 kg m^{-3} PD and 165% PCS; 12% MMC: 800 kg m^{-3} PD and 165% PCS; 14% MMC: 800 kg m^{-3} PD and 165% PCS).

(Table 3). As expected, the gas pressure was higher when panel density increased (Fig. 16a). This effect can be explained by the lower mat gas permeability resulting from a higher panel density. Similar effects were observed by Humphrey and Bolton (1989a).

An example of the evolution of gas pressure in the core against time for the three MMCs considered is given in Figure 16b. The results of the analysis of variance show that for a PCS of 165% and a density of 800 kg m^{-3}, MMC had a significant effect on GP_{max}, an MMC of 10% resulting in a significantly lower GP_{max} than an MMC of 14% (Table 10). The higher moisture content combined to the lower gas permeability associated with a higher density can explain the high GP_{max} obtained for a panel density of 800 kg m^{-3}.

The results obtained for ΔGP_{max} are presented in Table 11. The analysis of variance shows that panel density has a significant impact on ΔGP_{max} (Table 3). As shown in Fig. 17, a panel density of 800 kg m^{-3} resulted in a significant increase in gas pressure difference between mat surface and core (ΔGP_{max}). The lower gas permeability at a higher panel density can explain this phenomenon.

CONCLUSIONS

The first objective of this study was to measure MDF gas permeability as a function of density. The results show that MDF intrinsic gas permeability decreases by a factor of 1000 when

TABLE 10. *Results obtained for GP_{max} (kPa) for all combinations.*

Mat moisture content (%)	Press closing strategy (% of target panel thickness)								
	145			155			165		
	Nominal panel density (kg m^{-3})								
	650	725	800	650	725	800	650	725	800
10	33	60	91	35	60	92	32	57	83
	(3)	(5)	(18)	(2)	(5)	(8)	(4)	(8)	(12)
12	37	60	98	38	55	107	34	54	94
	(5)	(1)	(6)	(3)	(7)	(14)	(2)	(5)	(29)
14	32	72	99	38	57	107	35	66	103
	(5)	(2)	(15)	(6)	(3)	(13)	(7)	(10)	(17)

ΔGP_{max}: maximum gas pressure in the mat and core (kPa). Standard deviation for three replicates of each combination is given in brackets.

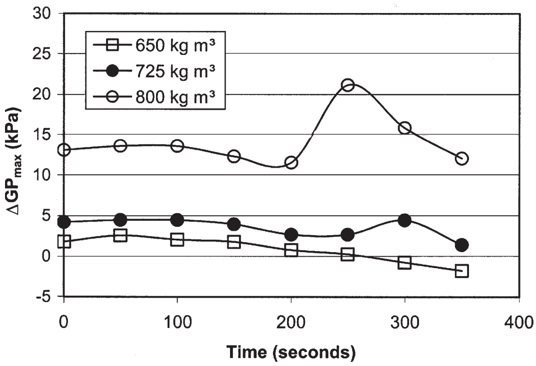

FIG. 17. Average gas pressure difference between mat surface and core (ΔGP_{max}) as a function of panel density.

panel density increases from 400 to 1150 kg m^{-3}. This result can be explained by the decreasing proportion of voids in the material as density increases.

The second objective of this study was to characterize the properties of MDF panels and temperature and gas pressure evolution in the MDF mat during hot pressing as a function of press closing strategy, mat moisture content, and panel density. The following conclusions can be made from the results we obtained within the range of conditions considered:

1. The modulus of elasticity and modulus of rupture increased significantly with an increase in mat moisture content, and panel density, and a decrease in press closing strategy. A higher surface density can explain this behavior. The optimum conditions for flexural properties were a press closing strategy of 145%, a mat moisture content of 14%, and a panel density 800 kg m^{-3}.
2. The internal bond strength increased significantly with mat moisture content and panel density. A highly significant interaction was observed between mat moisture content and panel density. A more efficient heat transfer to the core and a higher contact surface between fibers can explain this behavior. Press closing strategy had no significant impact on the internal bond strength for the range of conditions considered in this study. The optimum conditions for internal bond were a mat moisture content of 14% and a panel density of 800 kg m^{-3}.
3. The thickness swell after 24-h of immersion in water decreased significantly with an increase in panel density. Thickness swell increased with an increase in press closing strategy.
4. The time required to reach 100°C in the mat core decreased significantly with a decrease of press closing strategy. Mat moisture content had a significant impact on the time required to reach 100°C. A mat moisture content of 10% resulted in a lower time required to reach 100°C than for 12 and 14%. No clear explanation was found for this result. More investigation is required on this specific point.
5. The pressing parameters studied had no significant impact on the maximum temperature difference reached between mat surface and mat core.
6. The maximum gas pressure reached in the

TABLE 11. *Results obtained for ΔGP_{max} (kPa) for all combinations.*

Mat moisture content (%)	Press closing strategy (% of target panel thickness)								
	145			155			165		
	Nominal panel density (kg m^{-3})								
	650	725	800	650	725	800	650	725	800
10	4.1	6.3	8.6	2.5	0.8	31.3	1.5	0.8	8.6
12	1.3	1.3	39.4	1.0	1.3	1.8	1.3	1.0	8.8
14	17.4	7.1	40.1	2.0	10.8	4.3	4.0	17.2	52.2

ΔGP_{max}: maximum difference in gas pressure between mat surface and core (kPa).

core increased significantly with an increase in panel density. For a press closing strategy of 165% and a density of 800 kg m^{-3}, a significant increase of the maximum gas pressure occurs following an increase in mat moisture content. The higher moisture content combined to the lower gas permeability associated with a higher density can explain this effect.

7. The maximum difference in gas pressure between mat surface and core significantly increased for a density of 800 kg m^{-3}. The lower gas permeability at a higher panel density can explain this phenomenon.

ACKNOWLEDGMENTS

The authors are grateful to the Natural Sciences and Engineering Research Council of Canada (NSERC) for supporting this project under grant no. OGP0121954, to the International Tropical Timber Organization (ITTO) for a scholarship awarded to Rosilei A. Garcia, and to Uniboard Canada Inc., Panneaux MDF La-Baie panel plant for providing the wood fibers. We also thank Mr. Serge Plamondon for technical assistance.

REFERENCES

AMERICAN NATIONAL STANDARDS INSTITUTE (ANSI). 1994. Medium Density Fiberboard. National Particleboard Association. ANSI A208.2-1994. Gaithersburg, MO.

AMERICAN SOCIETY FOR TESTING AND MATERIALS (ASTM). 1996. Standard Test Methods for Evaluating Properties of Wood-Base and Particle Panel Materials. ASTM D1037-96a. Philadelphia, PA.

BOLTON, A. J., AND P. E. HUMPHREY. 1989. The hot pressing of dry-formed wood-based composites. Part III: Predict vapour pressure and temperature variation with time, compared with experimental data for laboratory boards. Holzforschung 43:265–274.

———, AND ———. 1994. The permeability of wood-based composite materials. Holzforschung 48: 95–100.

BOWEN, M. E. 1970. Heat transfer in particleboard during pressing. Ph.D. Thesis. Colorado State, USA. (In A. J. Bolton, and P. E. Humphrey. 1994. The permeability of wood-based composite materials. Holzforschung 48: 95–100.)

DAI, C., AND P. R. STEINER. 1993. Compression behavior of randomly formed wood flake mats. Wood Fiber Sci. 25 (4):349–358.

DENISOV, O. B., P. P. ANISOV, AND P. E. ZUBAN. 1975. Untersuchung der permeabilität von spanvliesen. Holztechnologie 16(1):10–14. (In A. J. Bolton, and P. E. Humphrey. 1994. The permeability of wood-based composite materials. Holzforschung 48:95–100.)

GEIMER, R. L. 1982. Dimensional stability of flakeboards as affected by board specific gravity and flake alignment. Forest Prod. J. 32(8):44–52.

———, AND J. H. KWON. 1999. Flakeboard thickness swelling. Part II. Fundamental response of board properties to steam injection pressing. Wood Fiber Sci. 31(1): 15–27.

GREUBEL, D., AND M. PAULITSCH. 1977. Investigations on dimensional changes in the plane of particleboard. III. Effect of raw material composition and processing variables on the dimensional changes in phenolic-resin bonded particleboard. Holz Roh-Werkst. 31(11):413–420. (In B. R. Vital, J. B. Wilson, and P. H. Kanarek. 1980. Parameters affecting dimensional stability of flakeboard and particleboard. Forest Prod. J. 30(12):23–29.)

HARLESS, T. E. G., F. G. WAGNER, P. H. SHORT, R. D. SEALE, P. H. MITCHELL, AND D. S. LADD. 1987. A model to predict the density profile of particleboard. Wood Fiber Sci. 19(1):81–92.

HATA, T., S. KAWAI, T. EBIHARA, AND H. SASAKI. 1993. Production of particleboards with a steam-injection. Press V. Effects of particle geometry on temperature behaviors in particle mats and on air permeabilities of boards. Mokuzai Gakkaishi 39(2):161–168.

HSE, G.-Y. 1975. Properties of flakeboards from hardwoods growing on southern pine sites. Forest Prod. J. 25(3): 48–53.

HSU, W. E. 1994. A brief review of dry-process fiberboard manufacturing. Forintek Canada Corp. 11 pp.

HUMPHREY, P. E., AND A. J. BOLTON. 1989a. The hot pressing of dry-formed wood-based composites. Part II: A simulation model for heat and moisture transfer, and typical results. Holzforschung 43:199–206.

———, AND ———. 1989b. The hot pressing of dry-formed wood-based composites. Part V: The effect of board size: Comparability of laboratory and industrial pressing. Holzforschung 43:401–405.

JOHNSON, S. E., AND F. A. KAMKE. 1994. Characteristics of phenol-formaldehyde adhesive bonds in steam injection pressed flakeboard. Wood Fiber Sci. 26(2):259–269.

KAMKE, F. A., AND L. J. CASEY. 1988a. Fundamentals of flakeboard manufacture: Internal-mat conditions. Forest Prod. J. 38(6):38–44.

———, AND ———. 1988b. Gas pressure and temperature in the mat during flakeboard manufacture. Forest Prod. J. 38 (3):41–43.

———, AND S. C. ZYLKOWSKI. 1989. Effects of wood-based panel characteristics on thermal conductivity. Forest Prod. J. 39(5):19–24.

LEHMANN, W. F. 1972. Moisture stability relationship in wood-base composition boards. J. Forest Prod. J. 22 (7): 53–59. (In A. J. Bolton, and P. E. Humphrey. 1994. The permeability of wood-based composite materials. Holzforschung 48:95–100).

LIHRA, T., A. CLOUTIER, AND S. ZHANG. 2000. Longitudinal and transverse permeability of balsam fir wetwood and normal heartwood. Wood Fiber Sci. 32(2):164–178.

MOSLEMI, A. A. 1974. Particleboard. Volume 2: Technology. Southern Illinois University Press, Carbondale and Edwardville, IL. 245 pp.

PARK, B. D., B. RIEDL, E. W. HSU, AND J. SHIELDS. 1999. Hot-pressing process optimization by response surface methodology. Composite and manufactured products. Forest Prod. J. 49(5):62–68.

PERRÉ, P., AND E. AGOUA. 2001. Propriétés de transfert massique dans les panneaux de MDF: Identification de paramètres morphologiques à partir de mesures de perméabilité et de diffusivité. Les Cahiers Scientifiques du Bois 2:105–117 (in French).

SIAU, J. F. 1995. Wood: Influence of moisture on physical properties. Virginia Polytechnic Institute and State University Press, Blacksburg, VA. 227 pp.

SMITH, D. C. 1982. Waferboard press closing strategies. Forest Prod. J. 32(3):40–45.

SOKUNBI, O. K. 1978. Aspects of particleboard permeability. M. Sc. Thesis. University of Wales, U. K. (In P. E. Humphrey, and A. J. Bolton. 1989a. The hot pressing of dry-formed wood-based composites. Part II: A simulation model for heat and moisture transfer, and typical results. Holzforschung 43:199–206).

SOSNIN, M. J. 1974. Untersuchung der elastizitat und verformbarkeit der spanvliese bei der spanplattenpressung. Holztechnologie 15 (1):45–48. (In F. A. Kamke, and L. J. Casey. 1988a. Fundamentals of flakeboard manufacture: Internal-mat conditions. Forest Prod. J. 38(6):38–44.)

VITAL, B. R., J. B. WILSON, AND P. H. KANAREK. 1980. Parameters affecting dimensional stability of flakeboard and particleboard. Forest Prod. J. 30(12):23–29.

WANG, S., AND P. M. WINISTORFER. 2000. Fundamentals of vertical density profile formation in wood composites. Part II. Methodology of vertical density formation under dynamic conditions. Wood Fiber Sci. 32(2):220–238.

WINISTORFER, P. M., W. W. MOSCHLER, G. S. WANG, AND E. DEPAULA. 2000. Fundamentals of vertical density profile formation in wood composites. Part I. In-situ density measurement of the consolidation process. Wood Fiber Sci. 32(2):209–219.

WOLCOTT, M. P., F. A. KAMKE, AND D. A. DILLARD. 1990. Fundamentals of flakeboard manufacture: Viscoelastic behavior of the wood component. Wood Fiber Sci. 22 (4):345–361.

XU, W., AND O. SUCHSLAND. 1998. Modulus of elasticity of wood composite panels with a uniform vertical density profile: A model. Wood Fiber Sci. 30(3):293–300.

ZUBAN, P. 1969. Effect of mat density and particle dimensions on the gas permeability of a chip mat. (In Russe). Lesoinzhenernoe delo i mekhanicheskaya tekhnologiya drevesiny. pp. 200–203. (In A. J. Bolton, and P. E. Humphrey. 1994. The permeability of wood-based composite materials. Holzforschung 48:95–100).